

Chip volume and cutting force calculations in 5-axis CNC machining of free-form surfaces using flat-end mills

Shan Luo¹ · Zuomin Dong¹ · Martin B.G. Jun¹

Received: 15 June 2016 / Accepted: 29 August 2016 / Published online: 19 September 2016
© Springer-Verlag London 2016

Abstract This paper presents two new methods and associated algorithms for numerically modeling chip geometry and calculating cutting force for parts with free-form surface during 5-axis CNC machining using a flat-end mill. Extending the computational geometry-based Alpha shape method that can only predict cutting chip geometry, a parallel slice local volume modeling approach has been added to predict cutting forces as well. To demonstrate the validity and capability of these new methods, simulation of the cutting and chip forming process of 5-axis CNC machining on a free-form surface has been carried out. Physical validation experiment in controlled conditions has been carried out on a 3-axis micro CNC machine with the two cutter rotation angles set to be zero. The predicted and measured cutting forces are in reasonably good agreement both in trend and magnitude. The presented chip volume and cutting force method can be used to perform cutting force estimation for generating optimal tool path and orientation during 5-axis milling. The method requires longer computational time than traditional analytical methods, but it supports the ultimate goal of chip volume modeling and calculation—accurate dynamics cutting force prediction.

Keywords Chip volume · Cutting force · 5-axis · Flat-end mill · Alpha shape · Free-form surface

1 Introduction

With the ability to potentially provide better tool accessibility to complex surfaces, produce more accurate curved surface, increase material removal rate, and reduce machine setup time, 5-axis CNC machining is widely used to produce various components with complex geometry [1]. However, it is challenging to calculate chip volume and cutting forces in 5-axis CNC machining using a flat-end mill due to the inclination and ration angles, the contact area between cutter and part surface changes all the time. Knowing values of removed chip volume and cutting forces can help choose optimal cutting parameters such as feed rate, depth of cut to improve the machining efficiency, and surface quality.

Chip thickness is a significant parameter to calculate chip volume and cutting forces. Chip thickness and cutting forces prediction for 5-axis CNC ball-end milling has been studied by many researchers [2]. However, very limited studies on 5-axis CNC machining using flat-end mills have been carried out [3], due to the complexity of cutter-part surface geometry interaction. A ball-end mill has constant curvature, therefore chip geometry is easier to obtain, while the curvature for flat-end mill at each cutter contact (CC) point varies with different tilt and lead angles during 5-axis machining. Thus, the discrete method for chip volume calculation with flat-end mill is much more complicated.

Undeformed chip shape can be constructed from the boundaries of instantaneous engagement domain between a flat-end mill and workpiece [4]. Accurately modeling the shape and volume of the removed material is a challenging task. There are two main approaches to calculate the removed chip volume [5]: (a) computation of swept volume by tool profile along NC trajectory and (b) implementation of the Boolean intersection and subtraction of the tool envelope with the workpiece. Workpiece based methods to calculate

✉ Martin B.G. Jun
mbgjun@uvic.ca

¹ Department of Mechanical Engineering, University of Victoria, Victoria, BC V8W 3P6, Canada

removed material in 5-axis machining is still a challenging due to the non-robust 3D Boolean subtraction operation and complicated process of updating workpiece [6]. Sweep volume is a tool representation method. It was introduced by Weinert [7] using a solid modeling technique. A moving frame in 5-axis tool motions was introduced for the solid sweep volume. Swept profiles were first generated along the NC trajectory. After moving the profiles, a closed-form envelope surface was created. This solid-based method can obtain much precise cutting volume than the discrete method. However, swept profiles are complicated to obtain as the cutter has both translational and rotational motions. Traditionally, the swept volume is obtained approximately by the sum of pure translational volume and pure rotational volume in 5-axis CNC machining. The results, even under the specified tolerance, are not exactly equal to the removed cutting volume. The depth of cut has not yet been included in the method, since swept volume only considers the top, bottom, and side of a milling cutter. Lee proposed a method to generate swept volume of a tool by calculating envelope profiles with Gauss map [8]. Yet, the approach is only applicable to convex set with piecewise C_1 -continuous motion. The trajectory of tool motion in the swept volume method is piecewise C_1 -continuous or smoothness. It requires that the first order derivative of the trajectory exists and is continuous. If the tool motion is smooth, the velocity of the tool can be used to get the swept profile. Otherwise, the swept profile cannot be found. Swept volume displays the shape of removed material and can be used for NC verification. However, it cannot produce the value of chip volume and chip thickness at each NC point to calculate cutting forces and select optimal cutting parameters. On the other hand, Ferry [9] generated a swept volume by collecting solid models of the tool together at various NC points along the tool trajectory. The swept volume was subtracted from the workpiece to get the finished part. The parallel slicing method (PSM) was used by Ferry to create cutter-workpiece engagement maps for 5-axis flank machining, with the information of engagement angles and depth of cut, which are the requirements for predicting cutting forces. The PSM can obtain the removed volume; however, it was a computationally inefficient approach to do Boolean operations for achieving the solid model of cutter-workpiece engagement.

In this paper, two numerical methods, the Alpha shape and the local parallel slice approaches, are proposed to calculate chip volume and cutting forces for a free-form surface during 5-axis CNC machining with a flat-end mill. A computational geometry-based method, Alpha shape, is applied to resolve the 3D cutter-workpiece intersection problems and obtain chip volume. The local parallel slice approach is used to obtain a cutter-workpiece engagement domain where the

cutting flutes entry and exit the workpiece and the depth of cut are required to predict cutting forces. These approaches are applicable in arbitrary tool orientations and consider depth of cut. Comparing with swept volume method, they are not restricted to be applied only in piecewise C_1 -continuous motions.

2 Chip volume calculation by the Alpha shape method

An Alpha shape defined in computational geometry is a family of piecewise linear simple curves in the Euclidean plane associated with the shape of a finite set of points [10]. The Alpha shape associated with a set of points is a generalization of the concept of the convex hull. The Alpha shape method is a well-established technique in computational geometry for triangulation, boundary, and area/volume of Alpha shape [11]. In this work, the Alpha shape method is used to model the volume and shape of removed chips during 5-axis milling. The model requires a chip boundary defined by a valid tool geometric outline at two continuous NC points.

2.1 The intersections of the tool motion at two continuous positions

In defining an Alpha shape chip profile, the geometric outline of the cutting tool is formed by the intersections of the tool at two adjacent cutter contact (CC) positions along the feed direction. Assuming a flat-end mill can be modeled as a cylinder, the chip geometry in 5-axis CNC machining can thus be modeled through the intersection of two cylinders at two continuous CC points, and the volume of the two intersected cylinders can be obtained. Since it is difficult to calculate the intersections of two arbitrary cylinders using close-form analytical model through translations and rotations, a numerical method has been used in this work to obtain the intersections of two arbitrary cylinders by dividing them into many thin layers along the z -axis direction. A vertical cylinder oriented at an arbitrary angle produces a projection as an ellipse onto a plane, as shown in Fig. 1. Therefore, the projections of two intersecting cylinders are two intersect ellipses on each layer. Intersections of two ellipses are then accumulated by layers, consisting intersections of the tool motion at two continuous CC positions.

For a flat-end mill, the cutter geometry is a cylinder, which can be represented as follows:

$$T = \begin{bmatrix} X \\ Y \\ Z \end{bmatrix} = \begin{bmatrix} r\cos\theta \\ r\sin\theta \\ z \end{bmatrix} \quad (1)$$

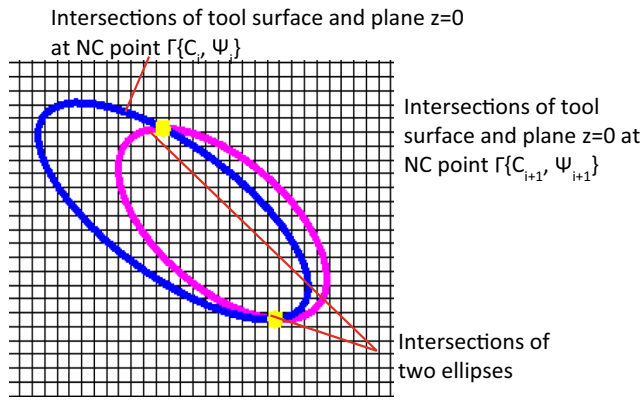


Fig. 1 Intersections of two ellipses for tool at two continuous NC positions

where, r is the tool radius, θ is the tool rotation angle about z -axis, $\theta \in [0, 2\pi]$, $z \in [h_1, h_2]$, and the length of the tool is defined by h_1 and h_2 . After rotation and translating, the new coordinate system $(X_{new}, Y_{new}, Z_{new})$ can be obtained [12]:

$$X_{new} = \cos\beta X - \sin\beta \cos\alpha Y + \sin\beta \sin\alpha Z + \Delta x \tag{2}$$

$$Y_{new} = \sin\beta X + \cos\beta \cos\alpha Y - \cos\beta \sin\alpha Z + \Delta y \tag{3}$$

$$Z_{new} = \sin\alpha Y + \cos\alpha Z + \Delta z \tag{4}$$

where, α and β are rotation angles about z and x axes; Δx , Δy , and Δz are translating distance along x , y , and z direction. Assuming the plane $z = 0$ is the top of the workpiece; the plane $z = h_1$ is the bottom of the tool at a NC point. After transformation, the projection of a cylinder is ellipse on the plane $z = h$ ($h \in [h_1, 0]$). For the ellipse, all z values are given as h . Substitute $Z_{C_{Anew}} = h$ into Eq. (4), it can be obtained that:

$$Z = \frac{h - \sin\alpha Y - \Delta z}{\cos\alpha} \tag{5}$$

Substituting Eq. (5) into Eqs. (1) and (3), the x and y values of points on the ellipse are derived as:

$$X_{\text{ellipse}} = \cos\beta X - \sin\beta \cos\alpha Y + \sin\beta \sin\alpha \frac{h - \sin\alpha Y - \Delta z}{\cos\alpha} + \Delta x$$

$$Y_{\text{ellipse}} = \sin\beta X + \cos\beta \cos\alpha Y - \cos\beta \sin\alpha \frac{h - \sin\alpha Y - \Delta z}{\cos\alpha} + \Delta y \tag{6}$$

For the i^{th} and $i^{th} + 1$ NC points: $\Gamma\{C_i, \Psi_i\}$ and $\Gamma\{C_{i+1}, \Psi_{i+1}\}$, they are denoted by $(x_i, y_i, z_i, \alpha_i, \beta_i)$ and $(x_{i+1}, y_{i+1}, z_{i+1}, \alpha_{i+1}, \beta_{i+1})$, respectively. Therefore, translating steps Δx_i , Δy_i , and Δz_i can be expressed as:

$$\Delta x_i = x_{i+1} - x_i, \Delta y_i = y_{i+1} - y_i, \Delta z_i = z_{i+1} - z_i \tag{7}$$

Substituting Eqs. (1) and (7) into Eq. (6), ellipse points on the plane $z = h$ as the tool motion at the i^{th} NC point can be obtained as:

$$X_{\text{ellipse}} = r \cos\theta \cos\beta_i - r \sin\theta \sin\beta_i \cos\alpha_i + \sin\beta_i \sin\alpha_i \frac{h - r \sin\theta \sin\alpha_i - (z_{i+1} - z_i)}{\cos\alpha_i} + x_{i+1} - x_i \tag{8}$$

$$Y_{\text{ellipse}} = r \cos\theta \sin\beta_i + r \sin\theta \cos\beta_i \cos\alpha_i - \cos\beta_i \sin\alpha_i \frac{h - r \sin\theta \sin\alpha_i - (z_{i+1} - z_i)}{\cos\alpha_i} + y_{i+1} - y_i \tag{9}$$

2.2 Chip outline determination

Two cases are considered for chip volume calculation as machining a complex surface.

The first case is a curve or a single toolpath machining. The second case is tool motions in two continuous tool paths. In a real free-form surface machining, there is a scallop height between two continuous tool paths due to the machining tolerance and tool compensation. In case 2, the chip volume is less than that in case 1. That is due to part of material in the current tool path has already been removed by the tool in the previous tool path. To calculate chip volume, two intersecting tool surfaces are firstly divided by layers to get their intersections (shown in Fig. 2b); two intersect ellipses which can be obtained from Eqs. (8) and (9), are then used to generate a crescent-shaped chip area along the feed direction in the Fig. 2a on each layer. Finally, intersections on all layers are collected to get the valid chip outline.

Figure 2a shows how chip geometry is generated. For case 1, a removed chip is created by the tool surface at two continuous NC points. More specifically, the intersection of tool outlines at two continuous NC points $\Gamma\{C_{i,j}, \Psi_{i,j}\}$ and $\Gamma\{C_{i+1,j}, \Psi_{i+1,j}\}$ represents removed material in the j^{th} tool path, denoted by a crescent area P_4P_5 along the feed direction. P_4 and P_5 are intersections of tool projections at NC points $\Gamma\{C_{i,j}, \Psi_{i,j}\}$ and $\Gamma\{C_{i+1,j}, \Psi_{i+1,j}\}$. For case 2, in the $j^{th} + 1$ tool path, as the tool moves from point $\Gamma\{C_{i+1,j}, \Psi_{i+1,j}\}$ to $\Gamma\{C_{i+1,j+1}, \Psi_{i+1,j+1}\}$, the removed chip area is $P_1P_2P_3$. P_1 is the intersection of tool projections on the plane $z = 0$ at two NC points $\Gamma\{C_{i,j+1}, \Psi_{i,j+1}\}$ and $\Gamma\{C_{i+1,j+1}, \Psi_{i+1,j+1}\}$; P_2 and P_3 are intersections of tool projections at $\Gamma\{C_{i,j+1}, \Psi_{i,j+1}\}$ and $\Gamma\{C_{i+1,j+1}, \Psi_{i+1,j+1}\}$ in the $j^{th} + 1$ tool path, and the tool projection at $\Gamma\{C_{i+1,j}, \Psi_{i+1,j}\}$ in the j^{th} tool path. Intersections on all layers are collected to get the valid chip outline shown in Fig. 2b.

2.3 Volume calculation by the Alpha shape method

The Alpha shape method defines the volume of a basic Alpha shape for a set of 3D points by Delaunay triangulation,

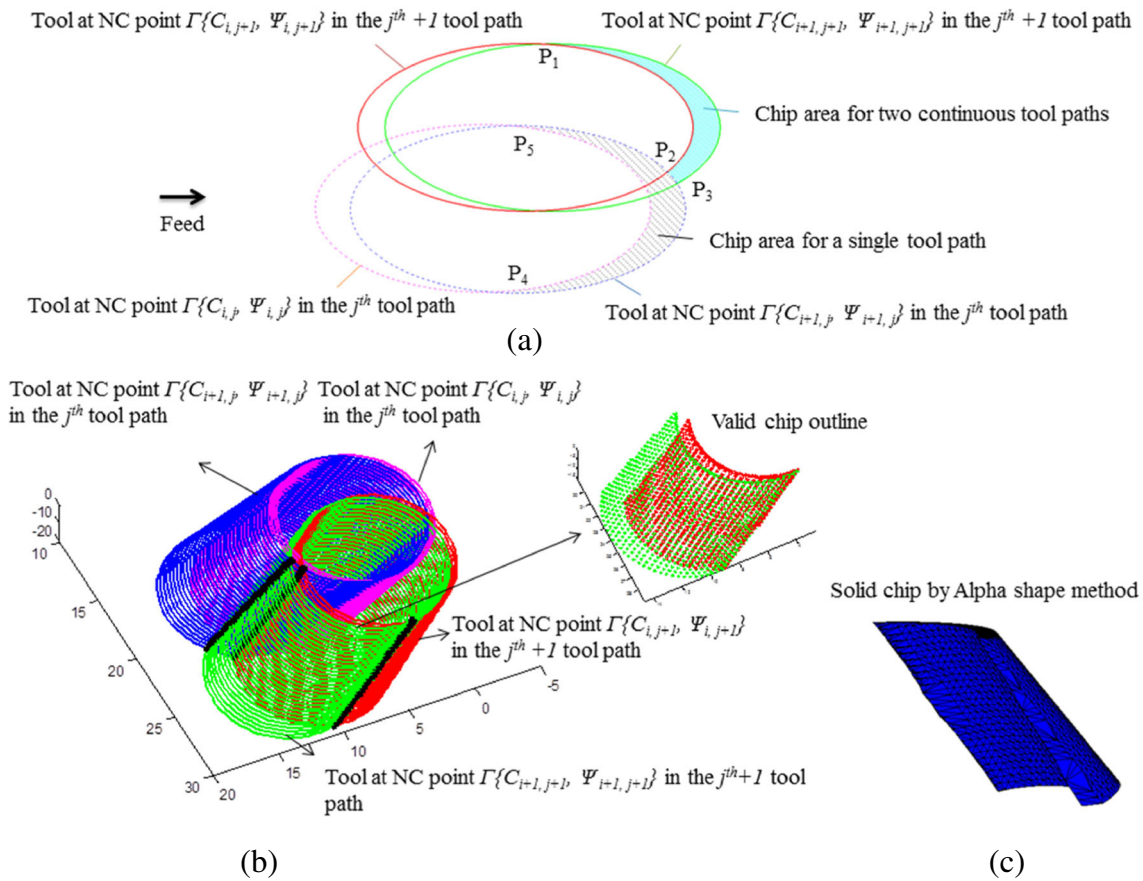


Fig. 2 a Chip area generation for different situations on the plane $z = 0$; b generation of the valid chip outline in two continuous tool paths; c a solid chip profile generated by the Alpha shape method

according to a probe radius, denoted by α . More specifically, Delaunay triangulation is carried out first to a 3D point set, and then the radius of circumcircles of simplices in triangulation is identified. If the radius of circumcircles is less than the probe radius, valid vertices of free boundary facets are found. Finally, the volume of Alpha shape can be calculated from the valid vertices. Solid Alpha shape created by Delaunay triangulation is composed by lots of tetrahedron. The volume of Alpha shape is obtained by accumulating volumes of all tetrahedrons which are part of the parallelepipeds. The volume of a tetrahedron can be represented by the volume of a parallelepiped.

In the Fig. 3, the volume of a 3D parallelepiped has been given by the scalar triple product of three vectors defined by four vertices A, B, C, D as follows:

$$V_{\text{parallelepiped}} = \vec{AD} \cdot (\vec{AB} \times \vec{AC}) \quad (10)$$

The volume of a tetrahedron (consisted by orange lines in the Fig. 3) is:

$$V_{\text{tetrahedron}} = \frac{V_{\text{parallelepiped}}}{6} \quad (11)$$

Alpha shape is an open source in MATLAB to give the area or volume of a basic Alpha shape for a 2D or 3D point set. In the algorithm, input is a probe radius and a coordinate matrix of size $N \times 3$, which are the 3D points consisting of the outline of a removed chip. Output is the volume and the plot of triangulation of the chip shape. In Fig. 2c, the removed chip is composed by many tetrahedrons, and the chip volume is obtained by the sum of volumes of all tetrahedrons, which are calculated using Eqs. (10) and (11).

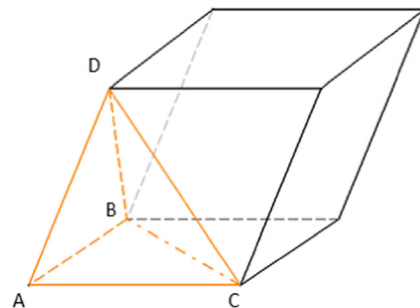


Fig. 3 Tetrahedron in a parallelepiped

3 Local parallel sliced method of chip volume and cutting force calculations

3.1 Chip load model

The Alpha shape method can be used to acquire the geometric profile of the removed chip. However, it cannot be used to calculate chip thickness and cutting forces. The chip profile points in Alpha shape method are the mesh points on the tool profile at two continuous NC points. A new approach called the local parallel slice method which extends the Alpha shape method—only for chip geometry and removal volume prediction is proposed to predict instant cutting forces for dynamic feed rate optimization. The local parallel sliced method divides the cutting tool into many slices perpendicular to the tool axis along the local coordinate system. It can calculate the chip thickness and cutting force by finding the intersections of the previous tool profile and a line passing the current tool center.

Figure 4a illustrates the determination of chip thickness in a 5-axis CNC machining using a flat-end mill. The tool is divided into many slices to get the chip volume by accumulating small parallelepipeds along the axial depth of cut and engagement angle. Let $O_i'-X_i'-Y_i'-Z_i'$ be the previous tool position and orientation, $O_i-X_i-Y_i-Z_i$ represent the current tool position and orientation after a distance of feed per tooth. In Fig. 4b, it

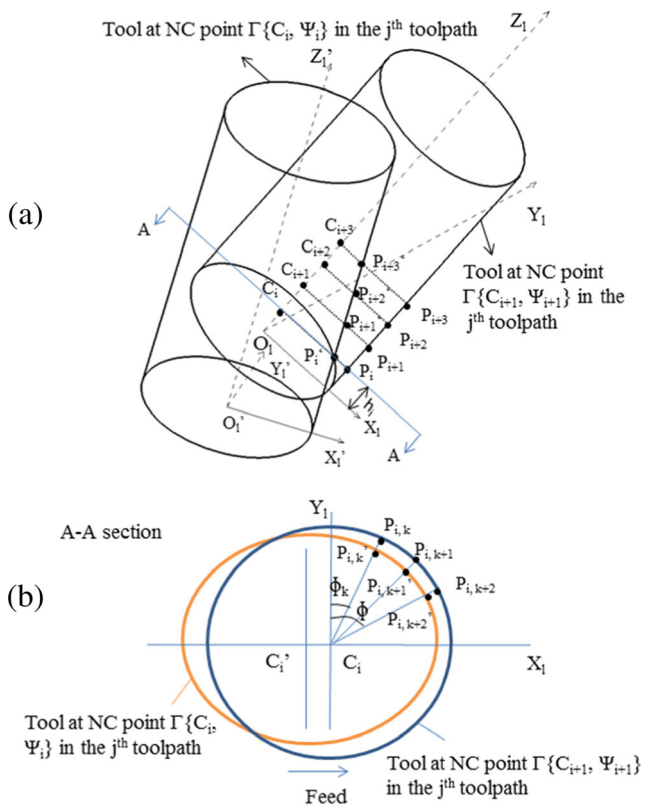


Fig. 4a Determination of instantaneous chip thickness: **a** tool motions at two adjacent NC points; **b** tool projections on A-A section

shows the instantaneous chip thickness distribution on the j^{th} layer. $P_{i,k}$ and $P_{i,k'}$ are the points on the current and previous tool's cutting edge determined by Eqs. (8) and (9); C_i and $C_{i'}$ are the current and previous tool centers; $C_i P_{i,k}$ is a vector line runs from the current tool center to the tool edge. $P_{i,k'}$ is the intersection of the line vector $C_i P_{i,k}$ and the previous tool edge. Chip thickness for the j^{th} flute can be defined as the distance between $P_{i,k}$ and $P_{i,k'}$, denoted by:

$$t_c(z, \phi, j) = \left| P(z, \phi, j) - P'(z, \phi, j) \right| \tag{12}$$

where z is the height along tool axis at the point P , ϕ is the engagement angle or immersion angle.

3.2 Chip volume by local parallel sliced method

On each slice, a polygon area is created by connecting current and previous tool edge points. Figure 5 shows a removal volume is divided into many layers along the direction which is perpendicular to the current tool axis. On each layer, the removal chip area is a polygon shape generated by connecting two neighboring edge points on the current and previous tool edges. A chip shape is composed by many parallelepipeds. The total chip volume is obtained by adding the volume of all parallelepipeds along the axial direction.

The equation of total chip volume is defined by:

$$V_{\text{total}} = \sum_{k=1}^{M-1} \sum_{i=1}^N P_{i,k} P_{i,k+1} \times P_{i,k} P_{i,k'} \times \Delta z \tag{13}$$

where M is the number of interval points on each layer, N is the number of slices; Δz is the integrating height along current tool axis.

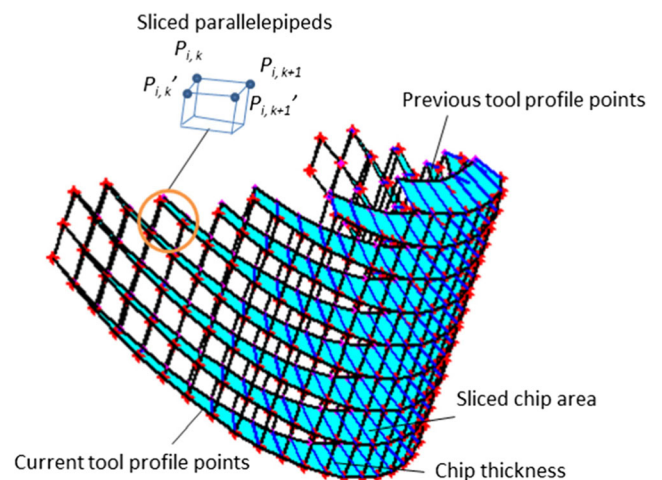


Fig. 5 A chip shape consists of sliced parallelepipeds

3.3 Cutter-workpiece engagement maps

A cutting force model requires getting engagement area by discretizing the cutter into slices in the tool coordinate system. The immersion angle ϕ in Fig. 4b is measured clockwise from the y -axis in local coordinate system.

The cutter-workpiece engagement maps [9] are generated by transforming a removal chip shape at a particular tool motion from global coordinate system to local coordinate system. The 3D chip shape, as illustrated in Fig. 5, is projected to the plane Y_lZ_l , which goes through the current tool axis. The boundaries of the engagement domain are the intersections of tool envelope at two continuous tool motions.

The engagement domain consists of many pieces of rectangles in Fig. 6, which is convenient to predict cutting forces. Each rectangle represents an immersion angle at a specified height along the tool axis. It is given by four parameters: ϕ_{st} , ϕ_{ex} , Δz , Z . ϕ_{st} and ϕ_{ex} are entry and exit angles; Δz is the integrating height or the height of a rectangle and Z is the distance from the tool tip to bottom of rectangles.

The number of layers and rectangles depend on the resolution defined by user. Figure 7 shows the engagement domain with different numbers of slice planes and interval points on each slice at the NC point # 300 in a single tool path machining. Figure 7a displays the removal volume is generated by nine slice planes with an integrating height of 0.33 mm; in Fig. 7b, it shows the engagement domain is divided into 15 slices. In this case, the distance between planes is 0.2 mm. The higher number of slices it is, the more accurate chip shape boundary there should be. The edge of engagement domain with high resolution in Fig. 7b is more smoothly and less “blocky” than that with lower number of slices in Fig. 7a. However, a high resolution case requires more significant computing time. It takes about 4 min to calculate chip volume and get engagement domain for over 700 NC points using a removal volume of nine slice planes. By increasing the number of slices to 15, the computing time was expanded to 8 min. The algorithm was written in Matlab. Matlab is inefficient in doing loop calculations compared to code written in C++ or C#. It is one reason why this method is time-consuming.

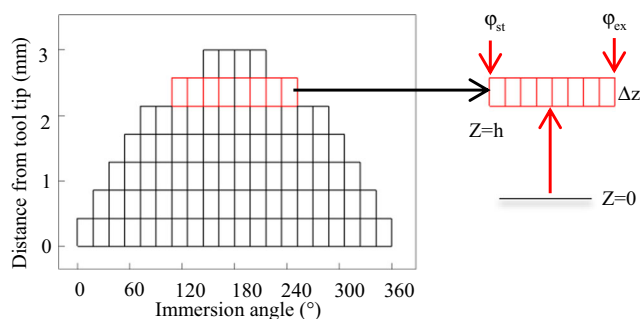


Fig. 6 2D cutter-workpiece engagement domain

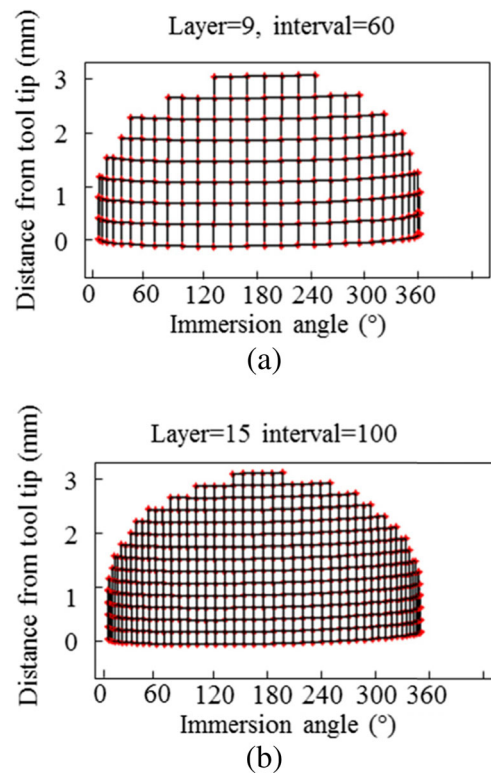


Fig. 7 Cutter-workpiece engagement domain: a nine slices with 60 interval points; b 15 slices with 100 interval points

Figure 8 shows how the sliced volume is gradually removed in a free-form surface machining. There are three NC points are demonstrated to the removed volume. The number of slices is different due to the varying depth of cut.

3.4 Cutting force model

Accurate modeling of cutting force is the focus of machine dynamics research, and it is the foundation for predicting cutting force to determine the optimal cutting parameters, such as feed rate and depth of cut, to improve the machining efficiency while meeting surface quality requirements.

The cutting force is normally modeled as three components, radial (F_r), axial (F_a), and tangential (F_t), shown in Fig. 9. They are expressed as [13–15]:

$$\begin{aligned} dF_r &= K_{rc} \times t_c(z, \theta, j) \times dz + K_{re} \times dz \\ dF_a &= K_{ac} \times t_c(z, \theta, j) \times dz + K_{ae} \times dz \\ dF_t &= K_{tc} \times t_c(z, \theta, j) \times dz + K_{te} \times dz \end{aligned} \tag{14}$$

where, K_{rc} , K_{ac} , and K_{tc} are the radial, axial, and tangential cutting force coefficients, respectively; and K_{re} , K_{ae} , and K_{te} are the edge force coefficients; dz is the integrating height, $t_c(z, \theta, j)$ is the instantaneous undeformed chip thickness at a NC point (x, y, z, α, β) , represented by Eq. (12).

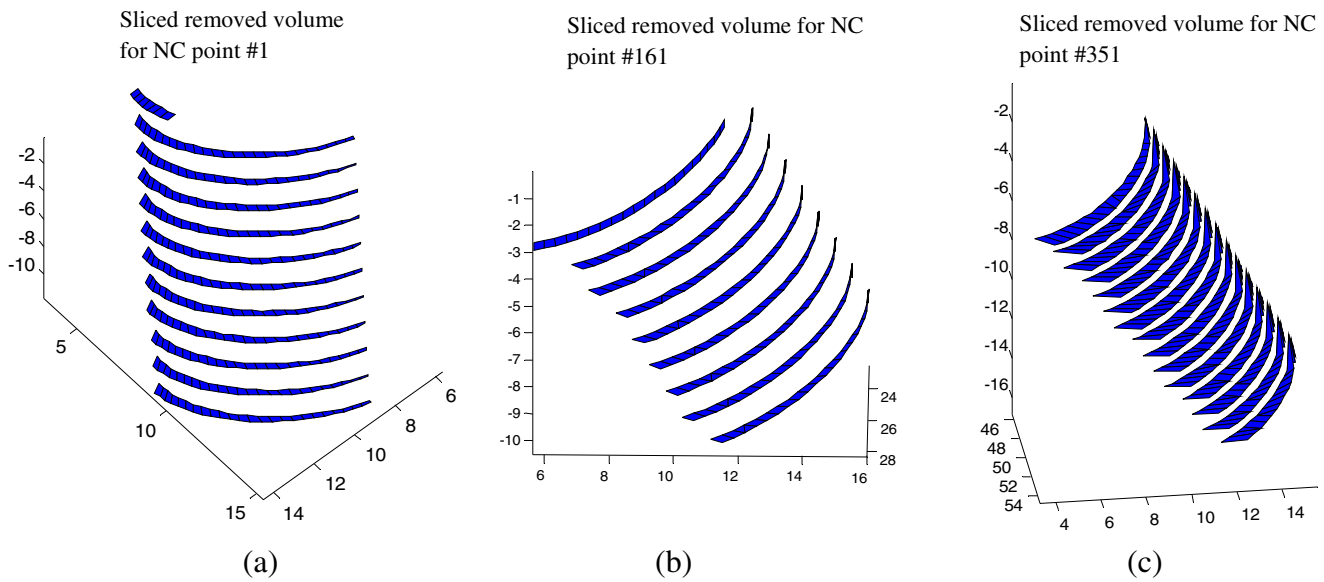


Fig. 8 a–c displays how the sliced volume is gradually removed in the free-form surface machining

The differential forces in local coordinate system (LCS) are transformed in x , y , and z direction by the following equation:

$$\begin{aligned} dF_x &= -dF_r \cos\phi - dF_t \sin\phi \\ dF_y &= dF_r \sin\phi - dF_t \cos\phi \\ dF_z &= dF_a \end{aligned} \tag{15}$$

Differential cutting forces for discretized engagement cutting edge elements are then summed by integrating the differential forces along the immersion angle and axial depth of cut to obtain the total forces for each given tool path segment.

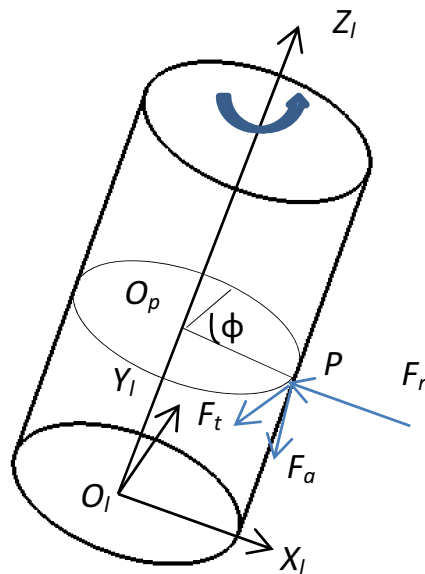


Fig. 9 Cutting geometry of a flat-end mill

4 Case studies and results

In this paper, a 5-axis CNC machine with swivel head configuration (AC type) is used to simulate tool motions. To display removed chips and get precise chip volume simulation, a free-form surface shown in Fig. 10a is machined by a four flutes flat-end mill, with a tool diameter of 10 mm. The workpiece size is with a length and width of 50 mm, respectively, and a height of 20 mm. The depth cut varying from 0.1 to 3 mm. Figure 10b shows the tool motions with various orientation angles in a pre-defined trajectory in MATLAB. The tool profiles are divided into two parts by a plane $z = 0$. Assuming the workpiece is under the plane $z = 0$. Depth of cut is the height from the center of the tool’s bottom to the top of the workpiece.

In the milling process, the cutting parameters are selected by the workpiece material and the tool size. The spindle speed is selected as 1000 rpm. For each revolution, the feed per tooth can be calculated by the following expression [16]:

$$f_t = \frac{f}{S \times N} \tag{16}$$

where, f is the feed rate, S is the spindle speed; N is the number of flutes.

The test NC program used in this paper is generated by commercial CAM software with 15,430 NC points. For each toolpath, there are approximately 1478 NC points employing the one-way toolpath. The toolpath generation method is followed by the iso-cusps method. Tool orientations are surface normal.

Removed chips are the part of the tool’s swept volume below the plane $z = 0$. It can be seen in the Fig. 2c, the shape of a removed chip is a 3D solid crescent, consisted by many

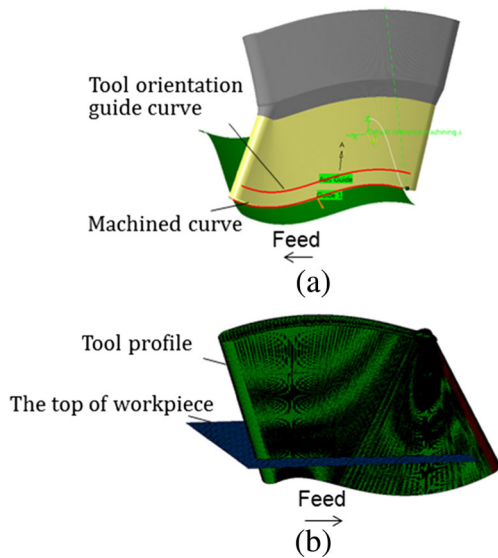


Fig. 10 **a** Simulation of machining a 3D curve on a free-form surface; **b** the simulation of tool motions in Matlab

tetrahedrons. In Fig. 11, the simulation of all chips in a single curve toolpath is generated through accumulating a crescent shape at each NC point by the Alpha shape method.

Figure 12 shows the comparison of chip volume by the Alpha shape method and the local parallel sliced method. It can be seen that the Alpha shape method gets more smooth and accuracy volume than the local parallel sliced method. Since the tetrahedron and triangulation are used in the Alpha shape method to calculate chip volume, which is more close to the real chip shape; while in the tool profile method, many rectangle blocks are accumulated to get chip volume. That is why the volume and cutting forces obtained from the local parallel sliced method look very “blocky”.

For each revolution, there are around 80 sampling points selected to calculate cutting forces. Cutting forces can be calculated from Eq. (15). Fig. 13 shows the simulation results of the instantaneous cutting forces in

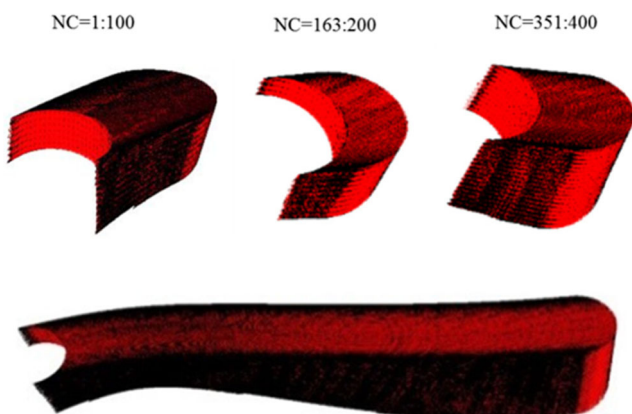


Fig. 11 Chip volume simulation for a single curve

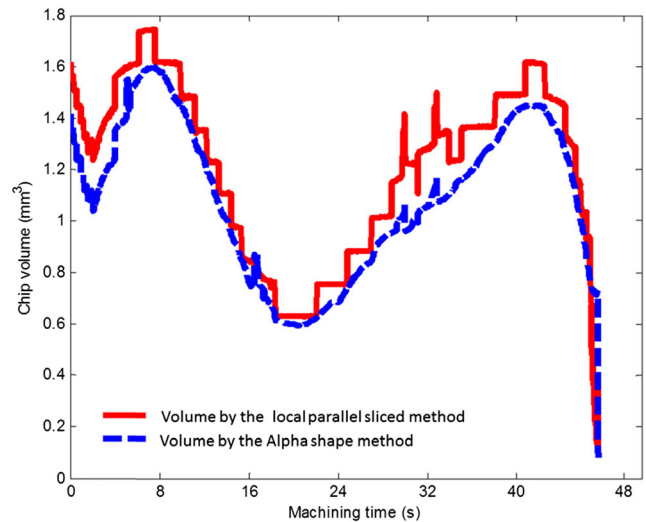


Fig. 12 Comparison of chip volume by the Alpha shape method and the local parallel sliced based method

x , y , and z directions changed with the rotation angles in five revolutions.

The resultant cutting force acting on the tool is calculated by:

$$R = \sqrt{F_x^2 + F_y^2 + F_z^2} \tag{17}$$

Figure 14 illustrates simulated cutting forces in x , y , and z directions and the resultant forces changing with machining times for the whole toolpath.

Comparing Fig. 12 and Fig. 14d, it can be seen that chip volume has similar changes to resultant cutting forces. Therefore, chip volume is another significant index in the machining process planning to select optimal feed rate, spindle speed, and depth of cut.

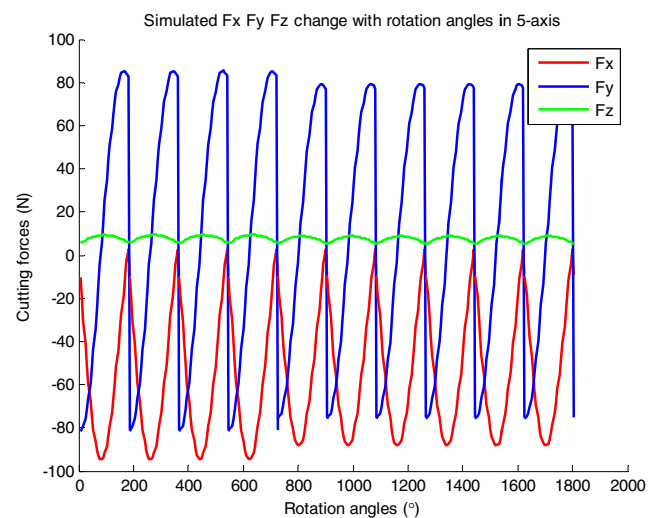
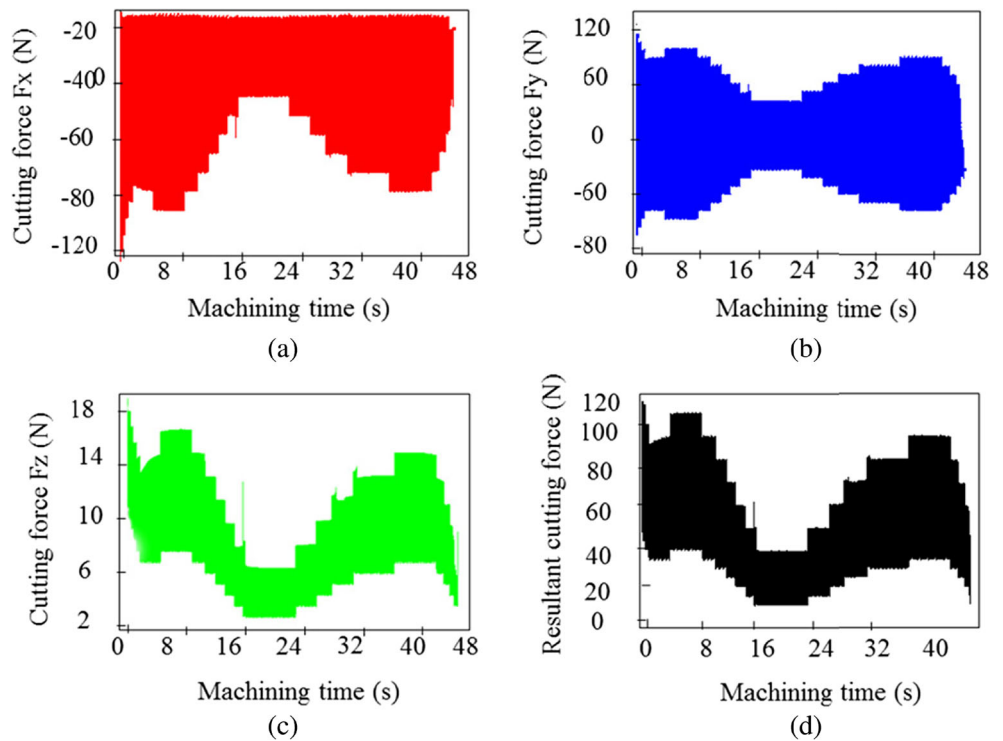


Fig. 13 Predicted cutting forces in x , y , and z directions for five revolutions in 5-axis CNC machining with a flat-end mill

Fig. 14 Simulated cutting forces for the whole toolpath: **a** F_x; **b** F_y; **c** F_z; **d** resultant forces



5 Experiment verification

For the validation of the proposed chip volume and cutting force modeling approaches, an experiment has been conducted on a free-form surface by using a flat-end mill. Due to the lack of a 5-axis CNC machine, a 3-axis CNC ALIO vertical micro-milling machine was used instead to verify the predicted cutting forces by enabling two rotational angles to be zeros. A Kistler table dynamometer (MiniDyn 9256C1) was used for measuring instantaneous cutting forces. Al 6061 workpiece was machined without lubricant by a 2-flute carbide flat-end mill with a diameter of 1/8". The experiment was carried out with varying axial depth of cut (0.1–1.2 mm) at 10,000 rev/min spindle speed and 0.02 mm feed per tooth. The sampling rate was 100 kHz, which is the maximum capacity of the DAQ board.

Figure 15 shows the comparison of measured and simulated cutting forces in three revolutions. It can be seen that the magnitudes of the predicted cutting forces in *x*, *y*, and *z* directions are in reasonably good agreement to the experimental ones if the runout effects are not considered. Cutting force calculations are based on the instantaneous chip thickness. The accuracy of predicted chip thickness can be guaranteed after the validation of simulated cutting forces. The discretized chip volume is obtained by the scalar triple product of chip thickness, integrating axial depth of cut, and radial edge contact length between two continuous interval points on each layer. Therefore, chip volume validation can be evaluated by measured cutting forces.

6 Conclusions

A general discussion for generating chip volume and predicting cutting forces in a 5-axis CNC machining with a flat-end mill has been presented in this paper. Two approaches of the Alpha shape and the local parallel sliced method have been used to obtain removed chip volume. The Alpha shape method provides an efficient and robust calculation of chip volume for arbitrary tool orientations because a series of complicated trigonometric equations to get intersections of tool

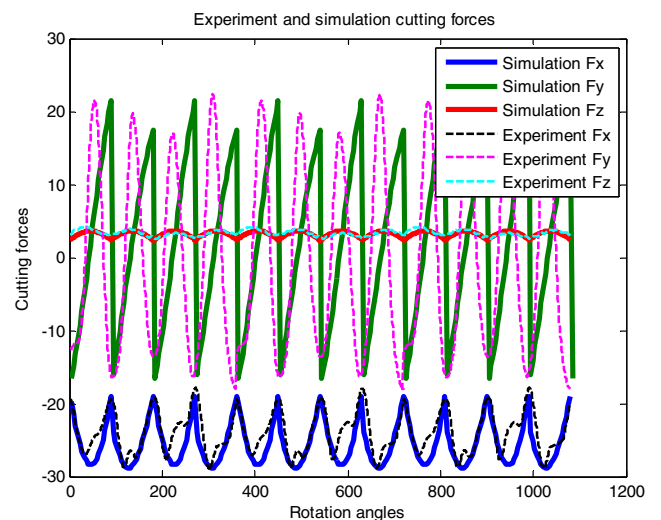


Fig. 15 Measured and predicted cutting forces with rotation angles in three revolutions

motions at two arbitrary positions are replaced by a numerical method. Although the Alpha shape method is able to calculate chip volume and display a solid chip shape with a fast computing time, it cannot be used to obtain chip thickness and predict cutting forces. The local parallel sliced method offers a new way to obtain cutter-workpiece engagement domain and cutting forces for a given NC file in 5-axis machining with a flat-end mill. This approach is robust to various types of cutters and sculpture surfaces without additional analysis. It also gives user a degree of flexibility to choose between computational speed, accuracy, and a combination of both by different resolutions.

To verify the proposed Alpha shape method and the local parallel sliced method and achieve precise chip volume simulation, the NC program for machining a free-form surface is developed to demonstrate cutting volumes. An experiment for the research of chip volume and cutting forces in 3-axis micro CNC machine was conducted. The simulation results for 5-axis machining were verified by machining experiments through specifying the two rotation angles to be zeros. Measured forces are shown in reasonably good agreement with simulated ones if the runout effects are ignored.

Acknowledgments Financial supports from the Natural Sciences and Engineering Research Council of Canada, the Technology Innovation Program (10053248, Development of Manufacturing System for CFRP (Carbon Fiber Reinforced Plastics) Machining) funded by the Ministry of Trade, Industry and Energy (MOTIE, Korea) and the China Scholarship Council are gratefully acknowledged. The authors would also appreciate and be grateful to the generous support and encouragement from our retired colleague, Professor Geoffrey W. Vickers.

References

1. Lasemi A, Xue DY, Gu PH (2010) Recent development in CNC machining of freeform surfaces: a state-of-the-art review. *Comput Aided Des* 42(7):641–654
2. Lamikiz A et al. (2004) Cutting force estimation in sculptured surface milling. *International Journal of Machine Tools & Manufacture* 44(14):1511–1526
3. Wang Y, Dong Z, Vickers G (2007) A 3D curvature gouge detection and elimination method for 5-axis CNC milling of curved surfaces. *Int J Adv Manuf Technol* 33(3–4):368–378
4. Ozturk B, Lazoglu I (2006) Machining of free-form surfaces. Part I: analytical chip load. *Int J Mach Tools Manuf* 46(78):728–735
5. Du S et al. (2005) Formulating swept profiles for five-axis tool motions. *International Journal of Machine Tools & Manufacture* 45(7–8):849–861
6. Lee S, Nestler A Virtual workpiece: workpiece representation for material removal process. *The International Journal of Advanced Manufacturing Technology* 58(5–8):443–463
7. Weinert K et al. (2004) Swept volume generation for the simulation of machining processes. *Int J Mach Tools Manuf* 44(6):617–628
8. Lee SW, Nestler A (2011) Complete swept volume generation, Part I: Swept volume of a piecewise C1-continuous cutter at five-axis milling via Gauss map. *Computer-Aided Design* 43(4):427–441
9. Ferry W, Yip-Hoi D (2008) Cutter-workpiece engagement calculations by parallel slicing for five-axis flank milling of jet engine impellers. *J Manuf Sci Eng* 130(5):51011
10. Edelsbrunner H, Kirkpatrick D, Seidel R (1983) On the shape of a set of points in the plane. *Information Theory, IEEE Transactions on* 29(4):551–559
11. Edelsbrunner H, Mucke EP (1994) Three-dimensional alpha shapes. *ACM Trans Graph* 13(1):43–72
12. Luo S (2015) Toolpath and cutter orientation optimization in 5-Axis CNC machining of free-form surfaces using flat-end mills. University of Victoria, Victoria, British Columbia
13. Boz, Y., H. Erdim, and I. Lazoglu (Modeling Cutting Forces for Five Axis Milling of Sculptured Surfaces: TRANS TECH PUBLICATIONS LTD.
14. Zhu RX, Kapoor SG, DeVor RE (2001) Mechanistic modeling of the ball end milling process for multi-axis machining of free-form surfaces. *Journal of manufacturing science and engineering-transactions of the ASME* 123(3):369–379
15. Altintas, Y.(2012) Manufacturing automation: metal cutting mechanics, machine tool vibrations, and CNC design Cambridge; New York
16. Mayor JR, Sodemann AA (2008) Intelligent tool-path segmentation for improved stability and reduced machining time in micromilling. *J Manuf Sci Eng* 130(3):31121